Dynamic Carboxylate/Water Networks on the Surface of the PsbO Subunit of Photosystem II

ARTICLE *in* THE JOURNAL OF PHYSICAL CHEMISTRY B · SEPTEMBER 2015

Impact Factor: 3.3 · DOI: 10.1021/acs.jpcb.5b06594

4 AUTHORS, INCLUDING:

Sara Capponi

University of California, San Francisco

16 PUBLICATIONS **73** CITATIONS

SEE PROFILE

THE JOURNAL OF PHYSICAL CHEMISTRY B

Article

pubs.acs.org/JPCB

Dynamic Carboxylate/Water Networks on the Surface of the PsbO Subunit of Photosystem II

Sebastian Lorch,[†] Sara Capponi,[‡] Florian Pieront,[†,§] and Ana-Nicoleta Bondar*[,†]

[†]Theoretical Molecular Biophysics, Department of Physics, Freie Universität Berlin, Arnimallee 14, D-14195 Berlin, Germany

[‡]Department of Physiology and Biophysics, University of California at Irvine, Medical Sciences I, Irvine, California 92697, United States

Supporting Information

ABSTRACT: Clusters of charged groups on the surface of proton-transfer proteins may participate in proton transfers. PsbO, an extrinsic subunit of photosystem II, is a carboxylate-rich protein part of an extensive hydrogen-bond network leading to the catalytic site. This raises the important question as to whether specific clusters of carboxylate groups on the surface of PsbO may directly assist transfer of protons from the catalytic site to the bulk. From molecular dynamics simulations of PsbO in aqueous solution, we find that, close to the surface of PsbO, the mobility of water molecules is lower than that for bulk water. At the site where PsbO docks and hydrogen bonds to photosystem II, water molecules have low mobility, and we identify a carboxylate cluster with persistent bridging of the carboxylates via short hydrogen-bonding water wires. This water-bridged carboxylate cluster could be important for proton transfer and binding of PsbO to photosystem II.

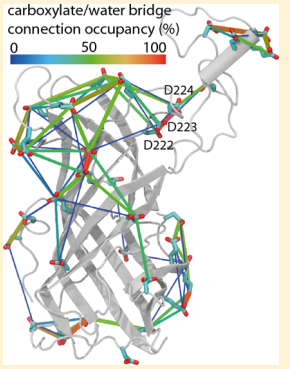

INTRODUCTION

Proton transfer proteins may use clusters of surface charged and polar groups as sites that can bind a proton and guide it to another site on the protein surface or to an internal proton acceptor.[1−3] Examples of proton transfer proteins thought to use proton-collecting groups, or antennas, include bacteriorhodopsin,[2,4,5] cytochrome *c* oxidase,[6,7] or the PsbO subunit of photosystem II.[8,9] In the AHA2 P-type ATPase plasma membrane proton pump, the primary proton donor/acceptor group is close to a carboxylate dyad exposed to the bulk phase.[10,11] Observations on the dielectric properties of lysozyme powders with different hydration levels were interpreted to suggest solvent-mediated movement of protons between protein sites,[12] and a potential proton wire connecting the active site to the solvent via water and protein groups was observed in the NAD(P)H:quinone oxidoreductase 1.[13] Their need to ensure efficient uptake/release of protons from/to the bulk phase could thus make proton-transfer proteins reliant on surface-exposed proton binding sites. Understanding the dynamics of protein/water hydrogen-bonding networks on the protein's surface can provide valuable insight into the key features of surface-exposed proton-binding sites.

PsbO is an excellent model system to assess the dynamics of surface-exposed carboxylate clusters. An extrinsic subunit of photosystem II, PsbO is thought to bind to the almost complete photosystem II monomer.[14] The high-resolution structure of the photosystem II complex from *Thermosynechococcus vulcanus*[15,16] indicates that PsbO has a β-barrel domain and long, unstructured loops and termini (Figure 1A), which appears compatible with NMR data indicating that PsbO has "both a well folded core and highly flexible regions."[17] Though its precise functional role remains unclear, PsbO appears to regulate functioning of photosystem II. Indeed, removal of PsbO from photosystem II leads to partial loss of the manganese ions from the catalytic center,[18] decreased oxygen production,[19] and perturbed dynamics of water at the active site[20] and of the reaction cycle.[21−23]

One mechanism by which PsbO could exert a functional role is by participating in proton-transfer networks. Measurements of the conformation of PsbO at different pH values lead to considerations of PsbO groups being potentially part of a proton-transfer wire,[24] and suggested that PsbO may have different conformations at pH values of 3.4−4.8 vs 6.0−9.5.[25] The temperature must also be taken into account when considering the potential implication of PsbO in proton transfers. At 200 K, PsbO undergoes conformational changes during the reaction cycle of photosystem II,[26] and the possibility was considered that one of its glutamic groups could deprotonate.[27] In contrast, deprotonation events could not be captured when FTIR measurements were performed at 277 K, which was interpreted to suggest that deprotonation of PsbO groups may occur only in part of the sample, or that deprotonation may be very fast.[28]

To begin to understand how PsbO may participate in proton transfer networks, it is important to consider an intriguing feature of PsbO: It has a high content of carboxylate groups (35 in the PsbO structure from *T. vulcanus*[15]), and some of these carboxylates are closely spaced as clusters[8,9] (Figure 1A and B).

Received: July 9, 2015
Revised: August 20, 2015

DOI: 10.1021/acs.jpcb.5b06594
J. Phys. Chem. B XXXX, XXX, XXX−XXX

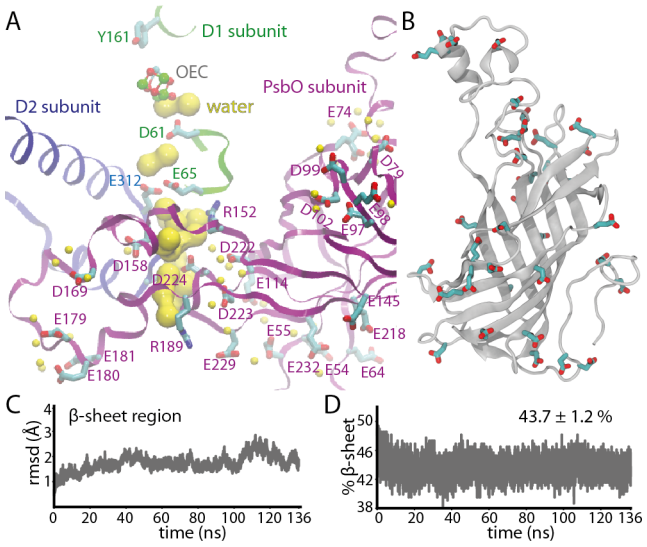

Figure 1. PsbO structure, interactions, and dynamics. (A) Carboxylate and water interactions at the binding interface of PsbO in photosystem II. We show a close view of the hydrogen-bonding network that extends from the PsbO group D224 to D61 of the D1 subunit. Water molecules of the hydrogen-bonding network are depicted as a yellow surface with a probe radius of 1.4 Å. The small yellow spheres are other water molecules within 3.5 Å of the carboxylate oxygen atoms shown explicitly. The following colors are used for protein atoms: carbon, cyan; oxygen, red; and hydrogen, white. Note that E74 has two possible orientations: D1-E65 and D2-E312 are within hydrogen-bonding distance.[9] Panel A is based in part on ref 9. (B) PsbO is a β-barrel protein whose surface contains numerous carboxylate groups. The protein is depicted as gray cartoons, with the Asp and Glu side chains shown as bonds. Panels (A) and (B) are based on the crystal structure from ref 15 (PDB ID: 3ARC, chain O). (C) Time series of the Cα rmsd for the β-sheet region of PsbO. (D) Time series of the percentage of the β-sheet structure relative to the total PsbO structure. The β-sheet structure was evaluated using STRIDE[81] within VMD.[69]

Importantly, in photosystem II, PsbO contributes to a hydrophilic region thought important as putative proton-transfer path.[9,29−31] In Figure 1, we illustrate the extended hydrogen-bonding network involving PsbO that leads close to the oxygen-evolving complex, OEC, where water molecules are split into molecular oxygen, protons, and electrons. This extended hydrogen-bonded network includes the potentially protonated D1-E65/D2-E312 pair[9] and D1-D61, an amino acid residue that may be implicated in proton transfer[29,32,33] (see Figure 1A). The important functional role of the extended hydrogen-bonding network is underlined by spectroscopy data indicating that D1-E65 and D2-E312 (Figure 1A) contribute to a hydrogen-bonding network that includes carboxylates whose pK_a value changes during the reaction cycle.[34,35] In the photosystem II from spinach, PsbO D157 mutants (D158 in *T. elongatus* PsbO, Figure 1) bind to photosystem II, but have their oxygen evolution activities reduced to ∼30% of the wild-type level.[36]

Close to D224, the surface of PsbO is rich in carboxylate groups: there is a cluster of carboxylates extending from the D224 region to E229 and the carboxylates close to E54/E64 (Figure 1A). The presence of closely spaced carboxylate groups on the surface of PsbO could be relevant for proton-transfer networks: It had been estimated that two acidic groups within ∼8−12 Å distance are associated with a high probability that a proton released from one site will move to the second acidic group, as compared to diffusing to the bulk.[37] And, data on acid−base proton transfer in aqueous solutions were interpreted to suggest up to five water molecules that separate the acid and the base, with most of the proton transfer events occurring at two to three separating waters,[38]that is, over distances of ∼6−8 Å.

The observations summarized above highlight the importance of understanding the dynamics of protein/water hydrogen bonding on the surface of PsbO. At room temperature, in solvent water, how do the PsbO carboxylates interact with each other and with water molecules? Waters close to a protein's surface were shown to have anomalous dynamics,[39] being slower than waters in the bulk;[40−43] hydrogen bonding[44] and orientational dynamics[45−47] of the water molecules are perturbed, and the dynamics of the protein hydration waters couple to the protein dynamics.[48,49]

To study the water hydrogen bonding of carboxylate groups on the surface of PsbO, we first performed an ∼136 ns simulation of PsbO in water with picosecond writing of the coordinates. This equilibrated trajectory of PsbO in water provided starting coordinate snapshots to probe the fast carboxylate/water dynamics by carrying out multiple simulations with femtosecond saving of the coordinates. We find that, on the ∼1 ps timescale, the surface of PsbO appears heterogeneous with respect to the dynamics of water molecules within its first hydration shell, and that hydrogen bonding of carboxylate pairs to water couples strongly to protein dynamics. The D224 region of PsbO has persistent carboxylate/water bridging that may be important for proton transfer and binding of PsbO to photosystem II.

METHODS

PsbO Simulation System. For the starting coordinates of PsbO, we used chain O from the Protein Data Bank (PDB[50]) crystal structure PDB ID: 3ARC.[15] We included the calcium ion and the 195 water molecules associated with chain O in the crystal structure. Cys19 and Cys44 were modeled as a disulfide bridge.[15,51] Hydrogen atoms were constructed using the HBUILD module of CHARMM.[52] All titratable groups were considered in their standard protonation states; that is, all Asp/Glu groups were negatively charged, Arg/Lys were positively charged, and the histidines were protonated on the Nε atom. The protein was placed in the center of the Cartesian coordinates, and overlapped with a box of water molecules. Solvent water molecules overlapping with crystal structure atoms were removed, and eight sodium ions were added for charge neutrality. The simulation system contained a total of 181.057 atoms.

Molecular Dynamics Simulations. The protein atoms were described using the CHARMM22 force field[53,54] with the CMAP correction,[55] and the water molecules with TIP3P.[56]

All simulations were performed with NAMD 2.9.[57,58] The simulation system was first subject to geometry optimization and heating from 0K to 300 K within 300 ps, using an integration time step of 1 fs. We continued with a production run using Langevin dynamics to maintain the temperature (T) constant at 300 K, and a Nosé−Hoover piston to maintain the pressure (P) at 1 bar.[59,60] A first 1 ns equilibration was performed with anisotropic pressure coupling; we then used, for the remaining of the simulations, isotropic pressure coupling. We used SHAKE[61] to constrain the bonds involving hydrogen atoms. We used a switch function between 8 and 12 Å for the short-range real-space interactions, and used the

DOI: 10.1021/acs.jpcb.5b06594
J. Phys. Chem. B XXXX, XXX, XXX−XXX

smooth particle mesh Ewald summation[62,63] to compute the Coulomb interactions. To integrate the equations of motion during the production run we used the reversible multiple time-step algorithm[64,65] with time-steps of 1 fs for the bonded forces, 2 fs for the short-range nonbonded forces, and 4 fs for the long-range electrostatic forces. Coordinates were saved every 10 ps during the first ∼50 ns, and each 1 ps throughout the end of the simulation at ∼136 ns. In what follows, this simulation is referred to as the reference *NPT* simulation.

Short *NVE* Simulations to Detect Dynamical Carboxylate/Water Bridges. Breaking and forming of bulk water hydrogen bonds occur very fast, on the subpicosecond-picosecond time scale;[44,46,66,67] the protein/water hydrogen bonds have a somewhat slower dynamics.[44] Pursuant to these considerations, for the analysis of the carboxylate/water bridges we performed additional simulations as follows. From the last 30 ns segment of the reference *NPT* trajectory, we took seven equally spaced snapshots. We denote these snapshots as Stop 1, ..., Stop 7, whereby Stop 7 is the last snapshot of the reference *NPT* simulation. Then, from each Stop, we generated short repeat simulations in the *NVE* ensemble (constant number of atoms, *N*, constant volume, *V*, and energy, *E*) with a coordinate saving step of 5 fs and integration step of 1 fs. Starting from Stop 1, ..., Stop 7, respectively, we generated 10 short *NVE* trajectories, 200 ps each (i.e., we generated 70 × 200 ps *NVE* trajectories).

To further test water bridge dynamics, starting from the Stop 6 coordinate set, we performed an additional set of 10 *NVE* simulations, 200 ps each. Furthermore, to test the coupling between protein and water bridge dynamics, starting from Stop 7 we also performed a set of 10 × 200 ps *NVE* simulations by keeping the protein fixed; these simulations are denoted as Stop 7-*f*. In total, we report here 90 × 200 ps *NVE* simulations.

Detecting Carboxylate/Water Bridges on the Surface of PsbO. We denote as carboxylate/water bridges a pair of D/E side chains, denoted as c_1/c_2, and 1−5 intervening water molecules that establish a hydrogen-bonding chain. Two groups are considered hydrogen bonded when the distance between the oxygen atoms is ≤3.5 Å and the angle H···O′···O″ ≤ 50°, where O′ is a water oxygen atom and O″ is either water or carboxylate oxygen.

To find the bridges, we derived an initial data set (set-1) of carboxylate pairs c_1/c_2 for which the shortest distance d between their carboxylate oxygen atoms is ≤30 Å in the starting crystal structure. In the second step, we analyzed the time-dependent trajectories to extract from set-1 a subset of the c_1/c_2 pairs (set-2) for which $d \leq 17$ Å. The cutoff distance of 17 Å was chosen based on test computations of water bridges in the reference *NPT* simulation. The list of c_1/c_2 pairs of set-2 is updated at each coordinate step by recalculating the c_1/c_2 distances from set-1.

A given c_1/c_2 pair gives four possible pairs of carboxylate oxygen atoms. To simplify the analysis of carboxylate/water bridges, for each c_1/c_2 pair we consider here only the carboxylate oxygen atoms within shortest distance.

To calculate the shortest path via hydrogen bonding water molecules that connects the carboxylic oxygen atoms of a c_1/c_2 pair from set-2, we scan the region between the two carboxylate-oxygen atoms to find hydrogen-bonding water molecules as summarized in Scheme 1. Briefly, we first find the water molecules within the overlap region of two spheres, the first sphere, with a radius of 3.5 Å, is centered on the carboxylate oxygen atom c_1; the second sphere, which is centered on the c_2 carboxylate oxygen atom, has a radius d_0 equal to the distance between c_1 and c_2. Water molecules within this first overlap region that satisfy the hydrogen bond criterion are then used for the second step of the search. For example, water molecule w_1, which hydrogen bonds to c_1, is used in the second step of the search, when we find the hydrogen-bonding water molecules within the overlap region of a 3.5 Å sphere centered on w_1, and a sphere centered on c_2 with a radius d_1 (Scheme 1). The scan is completed when a bridge of maximum five hydrogen-bonding water molecule is found. When such a bridge is not found, the c_1/c_2 pair is discarded from the current set-2. At a given moment in time, a c_1/c_2 pair may be connected by more than one bridge of same length (e.g., two one-water bridges).

Scheme 1. Schematic Representation of the Algorithm Used to Detect the Carboxylate/Water Bridges[a]

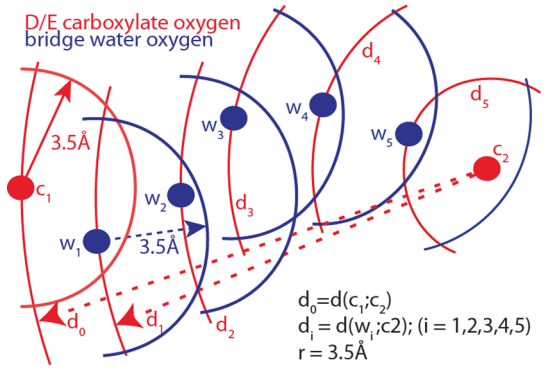

[a]Two carboxylate oxygen atoms of a c_1/c_2 carboxylate pair are selected for bridge detection if the distance between them is ≤17 Å. Of the four possible carboxylate oxygen pairs of each c_1/c_2 pair, we consider only the carboxyl oxygen atoms within the shortest distance. The scheme illustrates a search that results in finding a 5-water bridge between the carboxylate oxygen atoms c_1 and c_2.

The connection occupancy gives the percentage of the length of the analyzed trajectory during which the bridge is present. The connection length n of a water/carboxylate bridge gives the number of hydrogen bonding water molecules that intervene between the two carboxylate groups of the bridge. For the short *NVE* simulations generated at Stop 1, ..., Stop 7, unless otherwise specified we report connection occupancies and connection lengths averaged over the complete set of 10 × 200 ps *NVE* simulations of each Stop, using for analysis 20.000 equally spaced coordinate sets from each *NVE* simulation.

Water Mean Square Displacements (MSDs). The mean square displacement (MSD, in Å^2) of the water oxygen atoms during the time interval Δt was computed according to the equation

$$\mathrm{MSD}(\Delta t) = \langle |\boldsymbol{r}_i(t_0 + \Delta t) - \boldsymbol{r}_i(t_0)|^2 \rangle \quad (1)$$

where $\boldsymbol{r}_i$ is the position vector of the water oxygen atom i, and averaging is performed over the time origins t_0 and the number of water molecules. To calculate the water MSD(Δt = 1 ps) values, we used a 200 ps long *NVE* trajectory generated from Stop 6. Similar to the approach from ref 68, we considered successive shells centered at distances of 2, 3, ..., 12 Å from the protein, with a 4 Å thickness for each shell. We used as threshold a maximum of 6 Å for the linear displacement of water molecules included in the MSD calculation. Waters were

DOI: 10.1021/acs.jpcb.5b06594
J. Phys. Chem. B XXXX, XXX, XXX−XXX

assigned to the shells according to the $r_i(t_0)$ coordinate of their oxygen atom.

For data analyses, we used VMD 1.9.1[69] and our own scripts. All molecular graphics were prepared using VMD.[69]

RESULTS AND DISCUSSION

During the reference ~136 ns *NPT* simulation, the β-barrel core of the protein was largely stable (Figure 1C and D). The Cα root-mean-square distances (rmsd) relative to the starting crystal structure coordinates are ~2 Å (Figure 1C), and the percentage of β-sheet structure was stable at ~44% (Figure 1D). In what follows, we discuss the results on the dynamics of carboxylate/water hydrogen-bond dynamics.

Slow Water Dynamics close to the Surface of PsbO. To probe how interactions with protein groups affect water dynamics, we computed the MSD(Δt = 1 ps) values for water molecules. In Figure 2, we show the MSD of water molecules within the first hydration shell of each protein amino acid residue, and of waters further away from the protein. The MSD computations indicate that, within the data set considered, water molecules within the first hydration shell of PsbO appear to have slower MSD values as compared to bulk waters. But the extent to which the mobility of these water molecules is reduced varies across the protein surface (Figure 2A). At the D224 cluster the first-hydration shell waters appear somewhat slower than waters close to the nearby protein region. The MSD values appear to reach plateau values at ~10 Å (Figure 2B). This observation is compatible with data indicating that, for example, waters within ~10 Å of several different biomolecules have spectral characteristics different from bulk waters,[70] hydrogen bonding between waters within ~10 Å from a protein have longer lifetimes than bulk water,[71] or that the water diffusion coefficient within ~10−15 Å from myoglobin differs from bulk water values.[41]

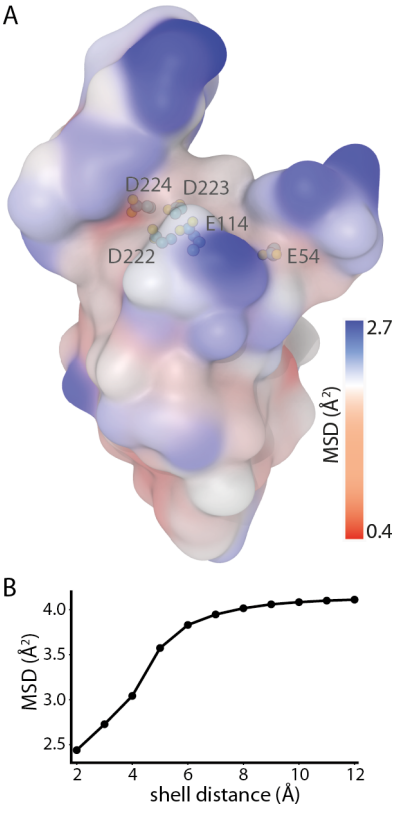

Figure 2. Slow water dynamics on the surface of PsbO. (A) Surface representation of PsbO, color-coded according to the MSD(Δt = 1 ps) values of waters of the first hydration shell, with MSD values ranging from 0.4 Å^2 (red) to 2.7 Å^2 (blue). The first hydration shell of an amino acid residue was defined as water molecules whose water oxygen atoms are within 3.5 Å distance from any of the heavy atoms of the amino acid residue. Atoms of the carboxylate side chains are shown as small spheres. (B) Water MSD values as a function of the distance from the protein surface. Note the gradual increase of the water MSD values for increasing distances to the protein surface. The MSD values were averaged over 3800 equally spaced time origins from a 200 ps long *NVE* trajectory generated from Stop 6.

Several Pairs of Surface Carboxylates Have Persistent Water Bridging. The PsbO structure used here has 35 Asp/Glu amino acid residues (Figure 1A and B). These carboxylate groups engage in extensive hydrogen bonding with water molecules (Figures 3−5). Throughout the last 70 ns of the reference *NPT* simulation, we find there are on average ~25 pairs of carboxylates that are bridged by 1−5 water molecules (Figures 3 and 4A, C). When averaged over the last 70 ns of the reference *NPT* simulation, the occupancies of most of these water-mediated connections are low (Figure 4B). That is, within 70 ns, the relative orientation of carboxylate side chains and, therefore, their water-mediated connections can change significantly (Figure 4D and E). Unexpectedly, however, for several pairs of carboxylates, we find relatively high overall probabilities of water bridging, for example, E84/E98, D205/E210, E218/E232, or D222/D224 (Figures 3, 4B, and 5). Inspection of the simulation indicates for the carboxylate groups of these pairs a consistent pattern whereby the carboxylates connect mostly via 1−3 water molecules (Figure 5). Albeit the length of the connection can change rapidly, on the picosecond time scale, overall a bridging configuration is sampled (Figure 5).

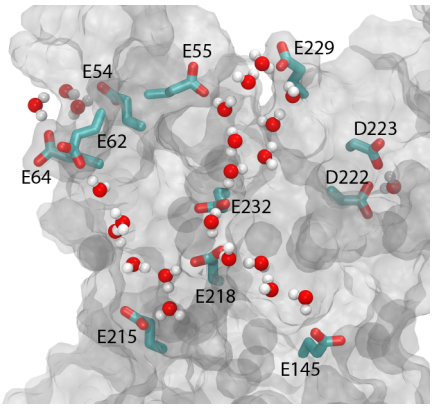

Figure 3. Illustration of selected carboxylate/water bridges on the surface of PsbO. Carboxylate/water bridges were identified using the protocol summarized in Scheme 1, based on a coordinate snapshot from one of the Stop 6 short simulations.

To estimate the dynamics of the carboxylate/water bridges on the nanosecond time scale, we performed the following analysis. For each of the D/E pairs within 30 Å distance (Figure 4C), we computed the connection probability for n = 1, 2, 3, 4, or 5 water molecules from the last 70 ns of the reference *NPT* simulation. Results from this connection occupancy computations are illustrated in Figure 4B. We then divided this last 70 ns fragment of the simulation into 7 consecutive segments, 10 ns each, and calculated the connection occupancy for each 10

DOI: 10.1021/acs.jpcb.5b06594
J. Phys. Chem. B XXXX, XXX, XXX−XXX

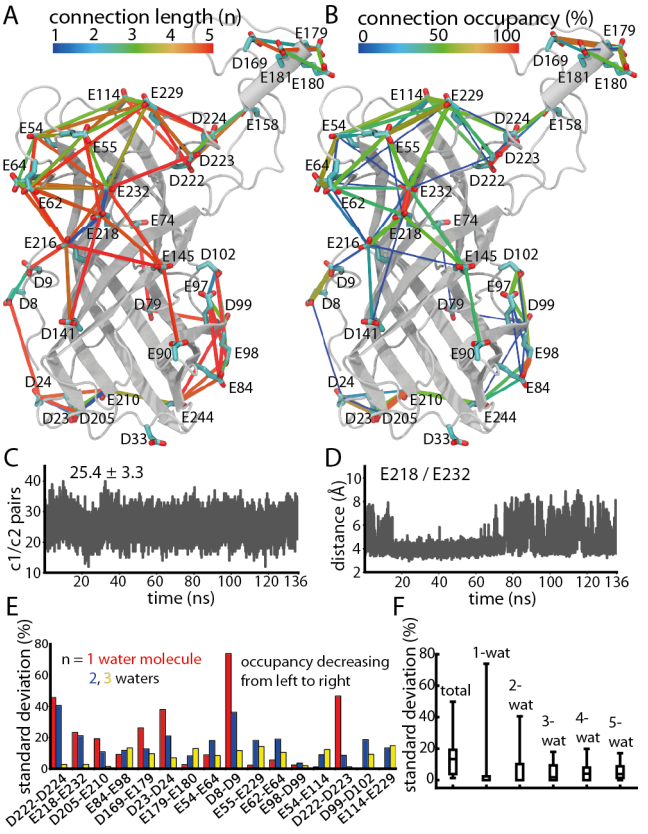

Figure 4. Dynamics of water bridges between specific pairs of carboxylate groups during the reference 136 ns simulation. (A, B) Illustration of water-bridged D/E pairs whose occupancy during the last 70 ns fragment of the reference *NPT* simulation is at least 1%. (A) Preferred connection length of specific carboxylate pairs. The colored lines interconnecting the D/E pairs indicate the preferred connection length n, which gives the number of waters in the bridge. Line color varies from blue (one water molecule) to red (five water molecules). (B) Occupancy of each connection throughout the last 70 ns of the reference *NPT* simulation. Note the high occupancy for the E218/E232 pair. (C) Time series of the number of D/E pairs whose carboxylate oxygen atoms are bridged by 1−5 hydrogen-bonding water molecules. Average value (25.4 ± 3.3 Å) was computed based on the last 70 ns of the *NPT* simulation. (D) Example of the dynamics of a c_1/c_2 pair. We monitor the shortest distance between the carboxylate oxygen atoms of E218 and E232. (E) Illustration of the standard deviation for connections via 1, 2, or 3 water molecules for selected carboxylate pairs with connection occupancy ≥ 70%. The large standard deviations for the occupancy of the D8-D9, D222-D223, or D222-D224 bridges arise largely from variations in the one-water connectivity. (F) Box plot of the standard deviations computed for all carboxylate/water bridges whose occupancy is at least 1% during the last 70 ns of the reference *NPT* simulation.

ns segment. This indicated that, for the pairs included in the test, most of the connection occupancies have standard deviations within 20−30%, though there are several outliers with significant standard deviations (Figure 4E and F). That is, on the 10 ns time scale, there can be significant changes in the water bridging of carboxylate pairs. The largest standard deviation, close to ∼80%, is observed for the one-water bridge connecting D8 and D9.

The significant differences between the bridge occupancies on the nanosecond time scales are likely explained by both carboxylate side chain and water dynamics. On the nanosecond time scale, the carboxylate groups of a pair can sample largely

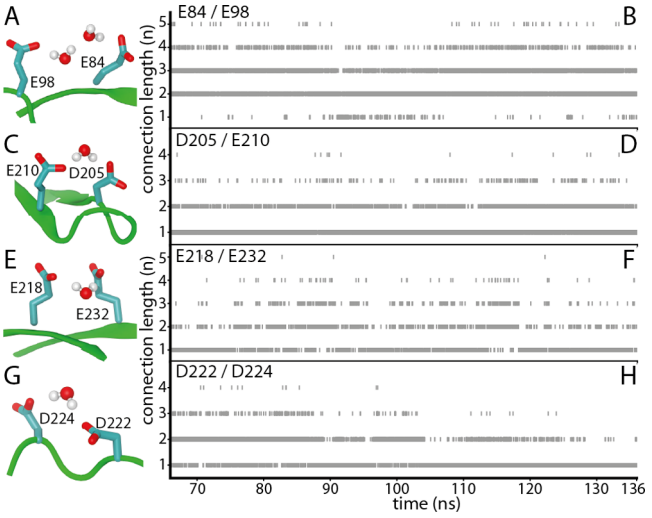

Figure 5. Dynamics of carboxylate/water bridges on the nanosecond time scale. Panels (A)−(H) give the molecular graphics and the corresponding time series of the connection length n of water bridges for the carboxylate pairs E84/E98 (panels A, B), D205/E210 (panels C, D), E218/E232 (panels E, F), and D222/D224 (panels G, H).

different relative orientations, which associates with fluctuations in the length of the hydrogen-bonding water chain; examples for carboxylate-pair dynamics and the corresponding water bridge dynamics are given in Figures 4D and 5F, respectively. For the D222/D224 pair, the relatively large standard deviations of the one- and two-water bridges on the nanosecond time scale (Figure 4E) are explained by the water bridging being mostly via one water during the last ∼40 ns of the simulation, as compared to frequent 2-water bridging during the first ∼30 ns used in the evaluation of the standard deviations (Figures 4E and 5H).

Coupling between Protein and Dynamics of Carboxylate/Water Bridges. The data summarized above on the connection occupancies computed from nanosecond-time scale data sets highlight the need to consider both the fast water dynamics and the slower dynamics of the protein groups. To this aim, we computed the water bridges based on short *NVE* trajectories with frequent, femtosecond writing, and accounted for protein dynamics by generating independent sets of *NVE* trajectories from seven different coordinate snapshots (Stops) taken from the reference *NPT* simulation.

To illustrate how the number of *NVE* simulations generated at each Stop may influence the results on the carboxylate/water bridge occupancies, in Table 1 we summarize the overall connection probabilities of 14 high occupancy c_1/c_2 pairs computed from 5 × 200, 10 × 200, or 20 × 200 *NVE* simulations generated from Stop 6. These test computations indicate similar connection occupancies regardless of the number of trajectories used. In what follows, we discuss the dynamics of carboxylate/water bridges based on independent averages computed from the 10 × 200 ps simulations started from Stop 1, ..., Stop 7. Connection occupancies for selected carboxylate/water bridges are summarized in Figure 6; additional data on occupancies computed for all Stops are given in Supporting Information Figure S1. We summarize below the general observations emerging from the *NVE* bridge occupancy data.

Carboxylate/water bridges tend to have higher occupancies when the number n of intervening water molecules is small, 1−

DOI: 10.1021/acs.jpcb.5b06594
J. Phys. Chem. B XXXX, XXX, XXX−XXX

Table 1. Average Connection Probabilities for Selected Carboxylate Pairs Computed from 5 × 200, 10 × 200, or 20 × 200 ps Short Simulations Started from Stop 6[a]

	data set used		
D/E pair	5 × 200 ps	10 × 200 ps	20 × 200 ps
D222/D224	99.6 (0.3)	99.3 (0.9)	99.3 (0.9)
D205/E210	95.7 (1.0)	94.6 (1.8)	94.8 (1.7)
D222/D223	95.1 (5.7)	95.5 (4.2)	96.2 (3.3)
E218/E232	92.5 (6.9)	93.4 (5.1)	94.4 (5.8)
E54/E64	92.4 (0.9)	92.7 (1.8)	91.4 (5.8)
E84/E98	91.1 (2.1)	90.0 (2.5)	90.2 (2.7)
D169/E179	91.9 (1.2)	89.4 (6.6)	90.9 (5.1)
D23/D24	89.9 (1.6)	88.3 (2.7)	88.2 (2.9)
E179/E180	77.9 (7.4)	81.3 (6.3)	78.8 (7.1)
E99/E102	77.9 (2.1)	78.4 (2.1)	75.8 (7.0)
D8/D9	78.0 (3.2)	78.2 (3.6)	79.6 (3.5)
E62/E64	76.3 (2.5)	77.8 (3.7)	77.9 (4.3)
E98/D99	69.4 (2.4)	72.4 (2.0)	73.8 (4.5)
E210/E244	69.3 (1.9)	70.1 (2.6)	70.0 (2.6)

[a]The D/E pairs are listed in decreasing order of their connection probability. Specific carboxylate groups are depicted in Figure 4A.

3 waters (see Figures 6 and S1). There are on average 3−4 one-water connections that have an occupancy ≥60%. For all Stops, the connections via 4−5 water molecules are dynamic.

At each of the 7 Stops considered, there is a high probability of connection via 1−2 water molecules between E218 and E232 (Figures 3 and 6), and of a one-water connection of D222 with D224 (Figure 6). D222 can further connect to D223 via high-occupancy one-water bridging (Stop 6, Figure S1F), or to E229 via low-occupancy, longer networks of 4−5 waters (Stop 5, Figure 6C and F). Likewise, D224 can further connect to D158 with high overall occupancy at Stops 1, 2, and 5 (Figures 6 and S1A, B, E), or via more dynamic, low occupancy bridges at Stops 4, 6, and 7 (Figure S1D, F, G). Near these carboxylate groups, E114 samples connections mostly with E54 and E229 (Stops 1, 4, 5, and 7), or E229 (Stops 2 and 3), and E218/E232 sample one-two water bridging at all Stops (Figures 6 and S1).

Another carboxylate cluster with persistent water bridging on the 200 ps time scale includes E84, E98, D99, and D102 (Figures 4A, 5A,B, and 6). At all Stops, E84 and E98 bridge mostly via 2−3 waters. E98 can further bridge to D99 via 2 waters, and D99 to D102 via 2−3 waters (Figures 6 and S1).

The picture that emerges from the analysis above of the carboxylate/water bridges is that the surface of PsbO has numerous carboxylate/water bridges, of which most are highly dynamic. Of the ∼25 carboxylate pairs that bridge via 1−5 waters at any given time (Figure 4C), a small number have persistent bridging via short hydrogen-bonding water chains. Intriguingly, D224, which in the photosystem II complex participates in a putative proton-transfer network (Figure 1A), is part of a cluster with persistent water bridging (Figure 6). Protein dynamics, that is, changes in the relative orientation of carboxylate groups (Figure 6D−F), couple to dynamics of carboxylate/water bridging (Figures 5, 6A−C, and S1).

To further dissect the coupling between protein and carboxylate bridge dynamics, we performed an additional set of 10 × 200 ps *NVE* simulations in which the protein coordinates were kept fixed to those of Stop 7 (Stop 7-*f*). We computed the water bridge occupancies at Stop 7-*f*, and compared the results with those obtained with a flexible protein at Stop 7 (Figure S1F and H). The dynamics of the D205/D210 bridge is largely the same at Stop 7-*f* vs Stop 7. At Stop 7-*f* the D222-D223 one-water bridge is very stable, and the E114/D222 water bridge is no longer sampled; the D222/D224 water bridge has somewhat smaller overall occupancy at Stop 7-*f*, and a higher percentage of bridging occurs via 2 waters (Figure S1H). The E216/E218 pair, which samples 1, 2, or 3 water bridging at Stop 7, with an overall occupancy of ∼69%, has ∼80% occupancy of 2 water bridging when the protein is fixed (Stop 7-*f*). In the flexible protein environment, E54 and E64 can bridge via 2−5 waters; when the protein is fixed, E54 and E64 bridge largely via 3 waters.

We interpret the observations on the carboxylate/water bridge dynamics with mobile vs fixed protein as an indication that protein dynamics may allow rapid rearrangements of the hydrogen-bonding water chains, making it more likely that a given carboxylate/water bridge samples different lengths of the water chain. Changes in the length of a carboxylate/water bridge require reorientation of water molecules. Our suggestion

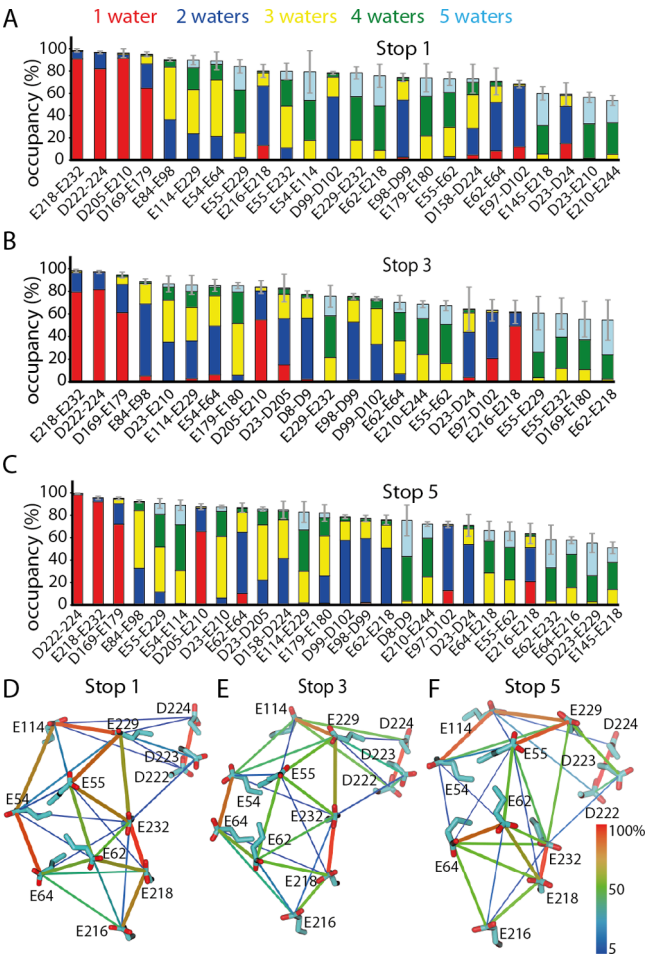

Figure 6. Coupling between protein dynamics and dynamics of carboxylate/water bridges. (A−C) Occupancy of carboxylate/water bridges computed as averages of 10 × 200 ps *NVE* simulations generated from, respectively, Stop 1 (A), Stop 3 (B), and Stop 5 (C). For simplicity, we depict only the carboxylate/water bridges that have an overall occupancy ≥50%. Additional data for water occupancies at all seven Stops, and for Stop 6-*f*, are given in Supporting Information Figure S1. The error bars indicate standard deviations for the overall connection occupancy of the c_1/c_2 pair, computed from each set of *NVE* simulations. (D−F) Molecular graphics illustrating selected carboxylate pairs and their connection probabilities computed at Stop 1 (D), Stop 3 (E), and Stop 5 (F).

DOI: 10.1021/acs.jpcb.5b06594
J. Phys. Chem. B XXXX, XXX, XXX−XXX

here that protein thermal motions could facilitate dynamic water bridging is compatible with recent molecular dynamics simulations indicating that, when the protein matrix is fixed, waters inside the protein translocon have retarded orientational dynamics,[72] and highlight the importance of accounting for protein and water dynamics when considering the functional role of PsbO in photosystem II.

CONCLUSIONS

We carried out all-atom molecular dynamics simulations of the PsbO subunit of photosystem II and performed extensive analyses to identify and characterize carboxylate groups that bridge via hydrogen-bonding water molecules. To rapidly identify the carboxylate/water bridges we relied on lists of carboxylate pairs within a cutoff distance, and used geometric criteria to calculate the probabilities of connections via water bridges of specific lengths (Scheme 1). This allowed us to identify and characterize the dynamics of the carboxylate/water hydrogen-bonding networks on the surface of PsbO.

The surface of PsbO hosts an extensive network of carboxylate/water hydrogen-bonding network (Figure 4A), of which most are highly dynamic on the nanosecond time scale (Figure 4B). This dynamic hydrogen-bonding network may help to rapidly propagate conformational changes from the OEC region to remote regions of PsbO (Figure 1A).

The ∼136 ns *NPT* simulation revealed that rapid changes in the connection length of a carboxylate/water bridge can occur on the picosecond-nanosecond time scale (Figure 4A, D, F), and that bridges can rearrange significantly on the 10 ns time scale (Figure 4E and F). These dynamics of the carboxylate/water bridges arise from changes in the mutual orientation of carboxylate side chains (Figure 4E and D), and from water dynamics, which are significant on the picosecond time scale (see Figure 2 and, for example, refs 46 and 73).

Since water motions are much faster than protein dynamics, we thought to dissect the coupling between protein dynamics and dynamics of the hydrogen-bonding water bridges. To this aim, we performed multiple *NVE* simulations started from seven different configurations, and with femtosecond writing of the coordinates. The computations indicate that, on time scales relatively short for protein dynamics, of 200 ps, several carboxylate groups engage in high-occupancy bridging via 1−2 waters; this includes D222/D224 (Figure 6). Carboxylate pairs that bridge via longer water chains, of 3−5 water molecules, are more dynamic, sampling water bridges of different length, although their overall bridging occupancy can be high (Figure 6A−C). When we kept the protein fixed, such reorientations of the carboxylate side chains could no longer contribute to the water bridge dynamics, and the picture of the dynamics of carboxylate/water bridging changed significantly. Whereas the occupancy of the short, high-occupancy carboxylate/water bridge D205/D210 barely responded to the protein being fixed, for some of the longer carboxylate pairs we observed increased preference for specific bridge lengths. That is, protein dynamics facilitates rapid reorientations of carboxylate side chains, which allows the carboxylate pairs to sample water bridges of various lengths, and exchange carboxylate bridge partners.

The D222/D223/D224 cluster has one or two high-occupancy bridges via 1−2 water molecules at each of the five protein Stops considered (Figure 6A−E). This engagement of water molecules in high-occupancy bridging is compatible with the observation from MSD calculations that, on the 1 ps time scale, water molecules in the first hydration shell of the D222/D223/D224 region have small MSD values (Figure 2A). We suggest that the short, stable carboxylate/water bridges of the D222/D223/D224 cluster (Figures 1A and 6) could be important structural and energetic determinants of a proton-transfer network, and/or for binding of PsbO to photosystem II.

Water molecules at protein interfaces can assist protein binding by, for example, mediating favorable protein/protein interactions,[74] or by providing a region where a reduced value of the dielectric constant enhances electrostatic interactions between proteins, thus favoring protein binding.[75] Based on our analyses of carboxylate/water hydrogen bonding, we suggest that the water molecules hydrogen-bonded to the D224 region (Figures 3, 4A, and 6) may provide a network of hydrogen bonds that help dock PsbO to photosystem II (Figure 1A).

Docking of PsbO to photosystem II likely changes the dynamics of PsbO. Instead of interacting with water molecules, as observed here for the free PsbO, some of the carboxylate groups could interact with protein groups from other protein subunits, either directly or via water hydrogen bonding. For example, in the crystal structure of photosystem II from *T. vulcanus*[15] PsbO groups such as D158, D169, or the D224 cluster, are close to the interface between PsbO and other protein subunits (Figure 1A). A potentially important interaction is the protein/water hydrogen-bonding cluster involving PsbO−D224 and groups from subunits D1 and D2: In the crystal structure of the complex,[15] there are water molecules close to PsbO D222, D223, and D224 (Figure 1A), such that D222 and D224 of PsbO, and D2-E310, appear part of a protein/water hydrogen-bonding cluster.[9] Detailed description of the dynamics of the PsbO interactions when bound to the membrane-embedded photosystem II would require prolonged simulations of the complex embedded in a hydrated lipid membrane.

Our simulations were performed on PsbO from *T. vulcanus*, which is a thermophilic cyanobacterium. Comparison of the amino acid sequences of PsbO from cyanobacteria and plants indicated important differences, including presence of a "cyano-loop" in cyanobacteria or, in plants, an insertion at the N terminus and presence of a segment rich in glutamate groups.[76,77] Without a high-resolution crystal structure of a plant photosystem II, the precise functional implications of specific differences in the amino acid sequences of PsbO from cyanobacteria vs plants are difficult to predict, particularly because the stoichiometry of PsbO binding could be different among these organisms. Instead of one PsbO copy per monomer as observed in the crystal structures of photosystem II from *T. vulcanus*[15] or *T. elongatus*,[32] photosystem II complexes from plants appear to have two copies of PsbO;[78,79] moreover, *Arabidopsins thaliana* has two isophorms of PsbO.[80] In spite of these differences, some PsbO groups appear conserved among plants and cyanobacteria. Based on the alignment of 33 PsbO sequences, it was observed that D158, D222, and D224 are highly conserved, whereas E229 has significant conservation in cyanobacteria;[76] conservation of these carboxylic groups is also observed in the alignment of the PsbO sequences from *T. elongatus* vs eight mesophilic cyanobacteria.[77]

Modeling proton transfer processes, with breaking and forming of chemical bonds, requires quantum mechanical treatment of the protein groups and water molecules that may directly participate in the proton transfer reaction. Although

DOI: 10.1021/acs.jpcb.5b06594
J. Phys. Chem. B XXXX, XXX, XXX−XXX

modeling of proton transfers was beyond the scope of our current work, we think that the approach we used could assist proton transfer calculations. The approach presented here can be used, for example, to derive a short list of carboxylate clusters of potential interest for further theoretical work with quantum mechanics, or to select groups for site-directed mutagenesis experiments. The analysis of surface protein/water hydrogen-bonding clusters could also be extended to include additional groups that could participate in dynamic protein/water hydrogen-bonding networks.

■ ASSOCIATED CONTENT

Supporting Information

The Supporting Information is available free of charge on the ACS Publications website at DOI: 10.1021/acs.jpcb.5b06594.

Average occupancies computed for Stops 1,...7, and for Stop 7-*f* (PDF)

■ AUTHOR INFORMATION

Corresponding Author

*E-mail: nbondar@zedat.fu-berlin.de.

Present Address

§F.P.: Düsseldorfer Straße 27, 10707 Berlin, Germany.

Notes

The authors declare no competing financial interest.

■ ACKNOWLEDGMENTS

This work was supported in part by the DFG Collaborative Research Center SFB 1078 "Protonation dynamics in Protein Function" (Project C4, to A-NB), funding from the Excellence Initiative of the German federal and state Governments, by the Freie Universität Berlin in support of SFB 1078, and an allocation of computing time from HLRN, the North-German Supercomputing Alliance (bec00063, to A.-N.B.). S.C. is supported in part by Grants GM74637 and GM86685 from the National Institute of Health. A.-N.B. and S.C. thank the International Office and the Center for Research Strategy of the Freie Universität Berlin for travel support. We acknowledge Abdal-Azim Al-Terkawi for generating some preliminary PsbO trajectories that were not included in the data analysis here. We thank Christopher Mielack, Holger Dau, and Martina Havenith for valuable discussions, and Jens Dreger for excellent technical support.

■ REFERENCES

(1) Gutman, M.; Nachliel, E. Time-Resolved Dynamics of Proton Transfer in Proteinous Systems. *Annu. Rev. Phys. Chem.* **1997**, *48*, 329−356.

(2) Checover, S.; Marantz, Y.; Nachliel, E.; Gutman, M. Dynamics of the Proton Transfer Reaction on the Cytoplasmic Surface of Bacteriorhodopsin. *Biochemistry* **2001**, *40*, 4281−4292.

(3) Gutman, M.; Nachliel, E.; Friedman, R. The Mechanism of Proton Transfer between Adjacent Sites on the Molecular Surface. *Biochim. Biophys. Acta, Bioenerg.* **2006**, *1757*, 931−941.

(4) Nachliel, E.; Gutman, M.; Kiryati, S.; Dencher, N. A. Protonation Dynamics of the Extracellular and Cytoplasmic Surface of Bacteriorhodopsin in the Purple Membrane. *Proc. Natl. Acad. Sci. U. S. A.* **1996**, *93*, 10747−10752.

(5) Riesle, J.; Oesterhelt, D.; Dencher, N. A.; Heberle, J. D38 Is an Essential Part of the Proton Translocation Pathway in Bacteriorhodopsin. *Biochemistry* **1996**, *35*, 6635−6643.

(6) Marantz, Y.; Nachliel, E.; Aagaard, A.; Brzezinski, P.; Gutman, M. The Proton Collecting Function of the Inner Surface of Cytochrome c Oxidase from *Rhodobacter sphaeroides*. *Proc. Natl. Acad. Sci. U. S. A.* **1998**, *95*, 8590−8595.

(7) Ädelroth, P.; Brzezinski, P. Surface-Mediated Proton-Transfer Reactions in Membrane-Bound Proteins. *Biochim. Biophys. Acta, Bioenerg.* **2004**, *1655*, 102−115.

(8) Shutova, T.; Klimov, V. V.; Andersson, B.; Samuelsson, G. A Cluster of Carboxylic Groups in PsbO Protein Is Involved in Proton Transfer from the Water Oxidizing Complex of Photosystem II. *Biochim. Biophys. Acta, Bioenerg.* **2007**, *1767*, 434−440.

(9) Bondar, A. N.; Dau, H. Extended Protein/Water H-Bond Networks in Photosynthetic Water Oxidation. *Biochim. Biophys. Acta, Bioenerg.* **2012**, *1817*, 1177−1190.

(10) Buch-Pedersen, M. J.; Pedersen, B. P.; Veierskov, B.; Nissen, P.; Palmgren, M. G. Protons and How They Are Transported by Proton Pumps. *Pfluegers Arch.* **2009**, *457*, 573−579.

(11) Guerra, F.; Bondar, A.-N. Dynamics of the Plasma Membrane Proton Pump. *J. Membr. Biol.* **2015**, *248*, 443−453.

(12) Careri, G.; Geraci, M.; Giansanti, A.; Rupley, J. A. Protonic Conductivity of Hydrated Lyzozyme Powders at Megahertz Frequencies. *Proc. Natl. Acad. Sci. U. S. A.* **1985**, *82*, 5342−5346.

(13) Faig, M.; Bianchet, M. A.; Winski, S.; Hargreaves, R.; Moody, C. J.; Hudnott, A. R.; Ross, D.; Amzel, L. M. Structure-Based Development of Anticancer Drugs: Complexes of NAD(P)H:Quinone Oxidoreductase 1 with Chemoterapeutic Quinones. *Structure* **2001**, *9*, 659−667.

(14) Rokka, A.; Suorsa, M.; Saleem, A.; Battchikova, N.; Aro, E.-M. Synthesis and Assembly of Thylakoid Protein Complexes: Multiple Assembly Steps of Photosystem II. *Biochem. J.* **2005**, *388*, 159−168.

(15) Umena, Y.; Kawakami, K.; Shen, J.-R.; Kamiya, N. Crystal Structure of Oxygen-Evolving Photosystem Ii at a Resolution of 1.9 Å. *Nature* **2011**, *473*, 55−60.

(16) Suga, M.; et al. Native Structure of Photosystem II at 1.95 Å Resolution Viewed by Femtosecond X-Ray Pulses. *Nature* **2014**, *517*, 99−103.

(17) Nowaczyk, M.; Berghaus, C.; Stoll, R.; Rögner, M. Preliminary Structural Characterization of the 33 kDa Protein (PsbO) in Solution Studied by Site-Directed Mutagenesis and NMR Spectroscopy. *Phys. Chem. Chem. Phys.* **2004**, *6*, 4878−4881.

(18) Miyao, M.; Murata, N. Role of the 33-kDa Polypeptide in Preserving Mn in the Photosynthetic Oxygen-Evolution System and Its Replacement by Chloride Ions. *FEBS Lett.* **1984**, *170*, 350−354.

(19) Bricker, T. M. Oxygen Evolution in the Absence of the 33-Kilodalton Manganese-Stabilizing Protein. *Biochemistry* **1992**, *31*, 4623−4628.

(20) Hillier, W.; Hendry, G.; Burnap, R. L.; Wydrzynski, T. Substrate Water Exchange in Photosystem II Depends on the Peripheral Proteins. *J. Biol. Chem.* **2001**, *276*, 46917−46924.

(21) Ono, T.; Inoue, Y. S-State Turnover in the O_2-Evolving System of $CaCl_2$-Washed Photosystem II Particles Depleted of Three Peripheral Proteins as Measured by Thermoluminiscence. Removal of 33 kDa Protein Inhibits S_3 to S_4 Transition. *Biochim. Biophys. Acta, Bioenerg.* **1985**, *806*, 331−340.

(22) Vass, I.; Ono, T.; Inoue, Y. Stability and Oscillation Properties of Thermoluminiscent Charge Pairs in the O_2-Evolving System Depleted of Cl^- or the 33 kDa Extrinsic Protein. *Biochim. Biophys. Acta, Bioenerg.* **1987**, *892*, 224−235.

(23) Miyao, M.; Murata, N.; Lavorel, J.; Maison-Peteri, B.; Boussac, A.; Etienne, A.-L. Effect of the 33-kDa Protein on the S-State Transitions in Photosynthetic Oxygen Evolution. *Biochim. Biophys. Acta, Bioenerg.* **1987**, *890*, 151−159.

(24) Shutova, T.; Irrgang, K.-D.; Shubin, V.; Klimov, V. V.; Renger, G. Analysis of pH-Induced Structural Changes of the Isolated Extrinsinc 33 Kilodalton Protein of Photosystem II. *Biochemistry* **1997**, *36*, 6350−6358.

(25) Weng, J.; Tan, C.; Shen, J.-R.; Zheng, X.; Xu, C.; Ruan, K. pH-Induced Conformational Changes in the Soluble Manganese-Stabilizing Protein of Photosystem II. *Biochemistry* **2004**, *43*, 4855−4861.

DOI: 10.1021/acs.jpcb.5b06594
J. Phys. Chem. B XXXX, XXX, XXX−XXX

(26) Hutchison, R. S.; Steenhuis, J. J.; Yocum, C. F.; Razeghifard, M. R.; Barry, B. A. Deprotonation of the 33-Kda Extrinsic, Manganese-Stabilizing Subunit Accompanies Photooxydation of Manganese in Photosystem II. *J. Biol. Chem.* **1999**, *274*, 31987−31995.
(27) Sachs, R. K.; Halverson, K. M.; Barry, B. A. Specific Isotopic Labeling and Photooxidation-Linked Structural Changes in the Manganese-Stabilizing Subunit of Photosystem II. *J. Biol. Chem.* **2003**, *278*, 44222−44229.
(28) Offenbacher, A. R.; Polander, B. C.; Barry, B. A. An Intrinsically Disordered Photosystem Ii Subunit, PsbO, Provides a Structural Template and a Sensor of the Hydrogen-Bonding Network in Photosynthetic Water Oxydation. *J. Biol. Chem.* **2013**, *288*, 29056−29068.
(29) Barber, J.; Ferreira, K.; Maghlaoui, K.; Iwata, S. Structural Model of the Oxygen-Evolving Centre of Photosystem II with Mechanistic Implications. *Phys. Chem. Chem. Phys.* **2004**, *6*, 4737−4742.
(30) Ishikita, H.; Saenger, W.; Loll, B.; Biesiadka, J.; Knapp, E.-W. Energetics of a Possible Proton Exit Pathway for Water Oxydation in Photosystem II. *Biochemistry* **2006**, *45*, 2063−2071.
(31) Gabdulkhakov, A.; Guskov, A.; Broser, M.; Kern, J.; Müh, F.; Saenger, W.; Zouni, A. Probing the Accessibility of the Mn_4Ca Cluster in Photosystem II: Channels Calculation, Noble Gas Derivatization, and Cocrystallization with DMSO. *Structure* **2009**, *17*, 1223−1234.
(32) Ferreira, K. N.; Iverson, T. M.; Maghlaoui, K.; Barber, J.; Iwata, S. Architecture of the Photosynthetic Oxygen-Evolving Center. *Science* **2004**, *303*, 1831−1838.
(33) Ho, F. M. Structural and Mechanistic Investigations of Photosystem II through Computational Methods. *Biochim. Biophys. Acta, Bioenerg.* **2012**, *1817*, 106−120.
(34) Service, R. J.; Hillier, W.; Debus, R. J. Evidence from FTIR Difference Spectroscopy of an Extensive Network of Hydrogen Bonds near the Oxygen-Evolving Mn_4Ca Cluster of Photosystem II Involving D1-Glu65, D2-Glu312, and D1-Glu329. *Biochemistry* **2010**, *49*, 6655−6669.
(35) Service, R. J.; Hillier, W.; Debus, R. J. Network of Hydrogen Bonds near the Oxygen-Evolving $MnCaO_5$ Cluster of Photosystem II Probed with FTIR Difference Spectroscopy. *Biochemistry* **2014**, *53*, 1001−1017.
(36) Popelkova, H.; Commet, A.; Yocum, C. F. Asp157 Is Required for the Function of PsbO, the Photosystem II Manganese Stabilizing Protein. *Biochemistry* **2009**, *48*, 11920−11928.
(37) Sacks, V.; Marantz, Y.; Aagaard, A.; Checover, S.; Nachliel, E.; Gutman, M. The Dynamic Feature of the Proton Collecting Antenna of a Protein Surface. *Biochim. Biophys. Acta, Bioenerg.* **1998**, *1365*, 232−240.
(38) Siwick, B. J.; Cox, M. J.; Bakker, H. J. Long-Range Proton Transfer in Aqueous Acid-Base Reactions. *J. Phys. Chem. B* **2008**, *112*, 378−389.
(39) Bizzarri, A. R.; Cannistraro, S. Molecular Dynamics Simulation Evidence of Anomalous Diffusion of Protein Hydration Water. *Phys. Rev. E: Stat. Phys., Plasmas, Fluids, Relat. Interdiscip. Top.* **1996**, *53*, R3040.
(40) Norin, M.; Haeffner, F.; Hult, K.; Edholm, O. Molecular Dynamics Simulations of an Enzyme Surrounded by Vacuum, Water, or a Hydrophobic Solvent. *Biophys. J.* **1994**, *67*, 548−559.
(41) Makarov, V. A.; Feig, M.; Andrews, B. K.; Pettitt, M. B. Diffusion of Solvent around Biomolecular Solutes: A Molecular Dynamics Simulation Study. *Biophys. J.* **1998**, *75*, 150−158.
(42) Sengupta, N.; Jaud, S.; Tobias, D. J. Hydration Dynamics in a Partially Denatured Ensemble of the Globular Protein Human α-Lactalbumin Investigated with Molecular Dynamics Simulations. *Biophys. J.* **2008**, *95*, 5257−5267.
(43) Bagchi, K.; Roy, S. Sensitivity of Water Dynamics to Biologically Significant Surfaces of Monomeric Insulin: Role of Topology and Electrostatic Interactions. *J. Phys. Chem. B* **2014**, *118*, 3805−3813.
(44) Bagchi, B. Water Dynamics in the Hydration Layer around Proteins and Micelles. *Chem. Rev.* **2005**, *105*, 3197−3219.
(45) Ahlström, P.; Teleman, P.; Jönsson, B. Molecular Dynamics Simulation of Interfacial Water Structure and Dynamics in a Parvalbumin Solution. *J. Am. Chem. Soc.* **1988**, *110*, 4198−4203.
(46) Sinha, S. K.; Bandyopadhyay, S. Local Heterogeneous Dynamics of Water around Lysozyme: A Computer Simulation Study. *Phys. Chem. Chem. Phys.* **2012**, *14*, 899−913.
(47) Laage, D.; Stirnemann, G.; Sterpone, F.; Rey, R.; Hynes, J. T. Reorientation and Allied Dynamics in Water and Aqueous Solutions. *Annu. Rev. Phys. Chem.* **2011**, *62*, 395−416.
(48) Conti Nibali, V.; D'Angelo, G.; Paciaroni, A.; Tobias, D. J.; Tarek, M. On the Coupling between the Collective Dynamics of Proteins and Their Hydration Water. *J. Phys. Chem. Lett.* **2014**, *5*, 1181−1186.
(49) Pizzitutti, F.; Marchi, M.; Sterpone, F.; Rossky, P. J. How Protein Surfaces Induce Anomalous Dynamics of Hydration Water. *J. Phys. Chem. B* **2007**, *111*, 7584−7590.
(50) Berman, H. M.; Westbrook, J.; Feng, G.; Gilliland, G.; Bhat, T. N.; Weissig, H.; Shindyalov, I. N.; Bourne, P. E. The Protein Data Bank. *Nucleic Acids Res.* **2000**, *28*, 235−242.
(51) Nikitina, J.; Shutova, T.; Melnik, B.; Chernyshov, S.; Marchenkov, V.; Semisotnov, G.; Klimov, V.; Samuelsson, G. Importance of a Single Disulfide Bond for the PsbO Protein of Photosystem II: Protein Structure Stability and Soluble Over-expression in *Escherichia coli*. *Photosynth. Res.* **2008**, *98*, 391−403.
(52) Brooks, B. R.; Bruccoleri, R. E.; Olafson, B. D.; States, D. J.; Swaminathan, S.; Karplus, M. CHARMM: A Program for Macromolecular Energy, Minimization, and Dynamics. *J. Comput. Chem.* **1983**, *4*, 187−217.
(53) MacKerell, A. D., Jr.; Bashford, D.; Bellott, M.; Dunbrack, R. L., Jr.; Evanseck, J. D.; Field, M. J.; Fischer, S.; Gao, J.; Guo, H.; Ha, S.; et al. All-Atom Empirical Potential for Molecular Modeling and Dynamics Studies of Proteins. *J. Phys. Chem. B* **1998**, *102*, 3586−3616.
(54) Brooks, B. R.; Brooks, C. L., III; MacKerell, A. D., Jr.; Nilsson, L.; Petrella, R. J.; Roux, B.; Won, Y.; Archontis, G.; Bartels, C.; Boresch, S.; et al. CHARMM: The Biomolecular Simulation Program. *J. Comput. Chem.* **2009**, *30*, 1545−1614.
(55) MacKerell, A. D., Jr.; Feig, M.; Brooks, C. L. I. Extending the Treatment of Backbone Energetics in Protein Force Fields: Limitations of Gas-Phase Quantum Mechanics in Reproducing Protein Conformational Distributions in Molecular Dynamics Simulations. *J. Comput. Chem.* **2004**, *25*, 1400−1415.
(56) Jorgensen, W. L.; Chandrasekhar, J.; Madura, J. D.; Impey, R. W.; Klein, M. L. Comparison of Simple Potential Functions for Simulating Liquid Water. *J. Chem. Phys.* **1983**, *79*, 926−935.
(57) Kale, L.; Skeel, R.; Bhandarkar, M.; Brunner, R.; Gursoy, A.; Krawetz, N.; Phillips, J.; Shinozaki, A.; Varadarajan, K.; Schulten, K. NAMD2: Greater Scalability for Parallel Molecular Dynamics. *J. Comput. Phys.* **1999**, *151*, 283−312.
(58) Phillips, J. C.; Braun, B.; Wang, W.; Gumbart, J.; Tajkhorshid, E.; Villa, E.; Chipot, C.; Skeel, R. D.; Kale, L.; Schulten, K. Scalable Molecular Dynamics with NAMD. *J. Comput. Chem.* **2005**, *26*, 1781−1802.
(59) Martyna, G. J.; Tobias, D. J.; Klein, M. L. Constant-Pressure Molecular-Dynamics Algorithms. *J. Chem. Phys.* **1994**, *101*, 4177−4189.
(60) Feller, S. E.; Zhang, Y.; Pastor, R. W.; Brooks, B. Constant Pressure Molecular Dynamics Simulation: The Langevin Piston Method. *J. Chem. Phys.* **1995**, *103*, 4613−4621.
(61) Ryckaert, J.-P.; Ciccotti, G.; Berendsen, H. J. C. Numerical Integration of the Cartesian Equations of Motion of a System with Constraints. Molecular Dynamics of N-Alkanes. *J. Comput. Phys.* **1977**, *23*, 327−341.
(62) Darden, T.; York, D.; Pedersen, L. Particle Mesh Ewald: An N X Log(N) Method for Ewald Sums in Large Systems. *J. Chem. Phys.* **1993**, *98*, 10089−10092.
(63) Essmann, U.; Perera, L.; Berkowitz, M. L.; Darden, T.; Lee, H.; Pedersen, L. G. A Smooth Particle Mesh Ewald Method. *J. Chem. Phys.* **1995**, *103*, 8577−8593.

DOI: 10.1021/acs.jpcb.5b06594
J. Phys. Chem. B XXXX, XXX, XXX−XXX

(64) Grubmüller, H.; Heller, H.; Windemuth, A.; Schulten, K. Generalized Verlet Algorithm for Efficient Molecular Dynamics Simulations with Long-Range Interactions. *Mol. Simul.* **1991**, *6*, 121−142.
(65) Tuckerman, M.; Berne, B. J.; Martyna, G. J. Reversible Multiple Time Scale Molecular Dynamics. *J. Chem. Phys.* **1992**, *97*, 1990−2001.
(66) Gutman, M.; Nachliel, E. The Dynamic Aspects of Proton Transfer Processes. *Biochim. Biophys. Acta, Bioenerg.* **1990**, *1015*, 391−414.
(67) Luzar, A.; Chandler, D. Hydrogen-Bond Kinetics in Liquid Water. *Nature* **1996**, *379*, 55−57.
(68) Heyden, M.; Havenith, M. Combining THz Spectroscopy and MD Simulations to Study Protein-Hydration Coupling. *Methods* **2010**, *52*, 74−83.
(69) Humphrey, W.; Dalke, W.; Schulten, K. VMD: Visual Molecular Dynamics. *J. Mol. Graphics* **1996**, *14*, 33−38.
(70) Sushko, O.; Dubrovka, R.; Donnan, R. S. Terahertz Spectral Domain Computational Analysis of Hydration Shell of Proteins with Increasingly Complex Tertiary Structure. *J. Phys. Chem. B* **2013**, *117*, 16486−16492.
(71) Ebbinghaus, S.; Kim, S. J.; Heyden, M.; Yu, X.; Heugen, U.; Gruebele, M.; Leitner, D. M.; Havenith, M. An Extended Dynamical Hydration Shell around Proteins. *Proc. Natl. Acad. Sci. U. S. A.* **2007**, *104*, 20749−20752.
(72) Capponi, S.; Heyden, M.; Bondar, A.-N.; Tobias, D. J.; White, S. H. Anomalous Dynamics of Water inside the SecY Translocon. *Proc. Natl. Acad. Sci. U. S. A.* **2015**, *112*, 9016−9021.
(73) Kropman, M. F.; Bakker, H. J. Dynamics of Water Molecules in Aqueous Solvation Shells. *Science* **2001**, *291*, 2118−2120.
(74) Levy, Y.; Onuchic, J. N. Water Mediation in Protein Folding and Molecular Recognition. *Annu. Rev. Biophys. Biomol. Struct.* **2006**, *35*, 389−415.
(75) Ahmad, M.; Gu, W.; Geyer, T.; Helms, V. Adhesive Water Networks Facilitate Binding of Protein Interfaces. *Nat. Commun.* **2011**, *2*, 261.
(76) de Las Rivas, J.; Barber, J. Analysis of the Structure of the PsbO Protein and Its Implications. *Photosynth. Res.* **2004**, *81*, 329−343.
(77) Williamson, A. K. Structural and Functional Aspects of the MSP (PsbO) and Study of Its Differences in Thermophilic Versus Mesophilic Organisms. *Photosynth. Res.* **2008**, *98*, 365−389.
(78) Popelkova, H.; Commet, A.; Kuntzleman, T.; Yocum, C. F. Inorganic Cofactor Stabilization and Retention: The Unique Functions of the Two PsbO Subunits of Eukaryotic Photosystem II. *Biochemistry* **2008**, *47*, 12593−12600.
(79) Popelkova, H.; Yocum, C. F. Psbo, the Manganese-Stabilizing Protein: Analysis of the Structure-Function Relations That Provide Insights into Its Role in Photosystem II. *J. Photochem. Photobiol., B* **2011**, *104*, 179−190.
(80) Murakami, R.; Ifuku, K.; Takabayashi, A.; Shikanai, T.; Endo, T.; Sato, F. Characterization of an Arabidopsis Thaliana Mutant with Impaired PsbO, One of the Two Genes Encoding Extrinsic 33-kDa Proteins in Photosystem II. *FEBS Lett.* **2002**, *523*, 138−142.
(81) Frishman, D.; Argos, P. Knowledge-Based Secondary Structure Assignments. *Proteins: Struct., Funct., Genet.* **1995**, *23*, 566−579.

DOI: 10.1021/acs.jpcb.5b06594
J. Phys. Chem. B XXXX, XXX, XXX−XXX